

# Thouless pumping in a driven-dissipative Kerr resonator array

S. Ravets,<sup>1,\*</sup> N. Pernet,<sup>1</sup> N. Mostaan,<sup>2,3,4</sup> N. Goldman,<sup>4,5</sup> and J. Bloch<sup>1</sup>

<sup>1</sup>*Université Paris-Saclay, CNRS, Centre de Nanosciences et de Nanotechnologies (C2N), 91120 Palaiseau, France*

<sup>2</sup>*Department of Physics and Arnold Sommerfeld Center for Theoretical Physics (ASC),*

*Ludwig-Maximilians-Universität München, Theresienstr. 37, D-80333 München, Germany*

<sup>3</sup>*Munich Center for Quantum Science and Technology (MCQST), Schellingstr. 4, D-80799 München, Germany*

<sup>4</sup>*CENOLI, Université Libre de Bruxelles, CP 231, Campus Plaine, B-1050 Brussels, Belgium*

<sup>5</sup>*Laboratoire Kastler Brossel, Collège de France, CNRS, ENS-PSL University, Sorbonne Université, 11 Place Marcelin Berthelot, 75005 Paris, France*

Thouless pumping is an emblematic manifestation of topology in physics, referring to the ability to induce a quantized transport of charge across a system by simply varying one of its parameters periodically in time. The original concept of Thouless pumping involves a non-interacting system, and has been implemented in several platforms. One current challenge in the field is to extend this concept to interacting systems. In this article, we propose a Thouless pump that solely relies on nonlinear physics, within a chain of coupled Kerr resonators. Leveraging the driven-dissipative nature of the system, we modulate in space and time the onsite Kerr interaction energies, and generate 1+1-dimensional topological bands in the Bogoliubov spectrum of excitations. These bands present the same topology as the ones obtained within the Harper-Hofstadter framework, and the Wannier states associated to each band experience a net displacement and show quantized transport according to the bands Chern numbers. Remarkably, we find driving configurations leading to band inversion, revealing an interaction-induced topological transition. Our numerical simulations are performed using realistic parameters inspired from exciton polaritons, which form a platform of choice for investigating driven topological phases of matter.

A one-dimensional system of non interacting electrons in a time-modulated periodic potential can show transport in absence of any external bias, a phenomenon known as geometric pumping. Strikingly, there exists modulation protocols where the electron motion is quantized in direct connection to the topology of the 1+1-dimensional (1+1D) bands that the system outlines during the protocol, in analogy to the quantum Hall effect [1]. In the case of filled bands, electrons move during a pump period by an integer number of unit cells equal to the sum of the Chern numbers of the filled bands [2]. Noteworthy, as quantized transport is intrinsically linked to the band structure, it can be accessed by monitoring the motion of the Wannier states. This way, Thouless pumping can also be accessed in bosonic systems.

The development of synthetic experimental platforms, providing exquisite control over the system parameters, has enabled experimental demonstrations of Thouless pumping. Examples include cold atoms confined in tunable optical lattices [3–5] or coupled to a cavity field [6], photons in coupled waveguides [7–9], plasmons in plasmonic waveguides [10], or mechanical excitations in metamaterials [11] or waveguides [12].

The picture gets even richer when considering interacting particles [13]. Interactions can induce topological pumping [14, 15], or lead to its breakdown [16, 17] depending on the interaction strength. Nonlinear solitonic waves on top of a Thouless pump have shown to exhibit quantized transport [18–22]. Thouless pumping has been proposed as a way to channel multiphoton quan-

tum states [23, 24]. Remarkably, interactions in bosonic systems are also known to renormalize the band structure for the elementary Bogoliubov excitations [25], and have been shown to induce non trivial topology in the Bogoliubov bands of an otherwise trivial system [26, 27]. To the best of our knowledge, the question whether one can organize a Thouless pump for the Bogoliubov modes of an interacting bosonic system remains unexplored so far.

In this letter, we propose an optically driven topological pump that entirely relies on the optical nonlinearity in a 1D array of driven-dissipative Kerr resonators. We consider a protocol where an optical drive is periodically distributed across the lattice sites with adiabatic time-periodic intensity modulation. Because of the Kerr nonlinearity, this protocol induces a modulation of the lattice onsite energies, proportionally to the local photon number. As a result, topological bands akin to Harper-Hofstadter bands emerge in the 1+1D Bogoliubov spectrum of excitations and Thouless pumping of the Wannier states is demonstrated. Moreover, we show that anharmonicity in the modulation protocol may induce topological transitions. We anticipate that this protocol could be implemented using exciton polariton lattices [28, 29], as this platform combines a giant Kerr nonlinearity with the ability to image Bogoliubov excitations both in real and k-space [30–33]. We therefore base our numerical simulations on realistic parameters that are relevant for the exciton polariton platform.

We consider an infinite periodic chain of identical Kerr resonators with constant couplings along the chain (see Fig. 1a). The linear part of the Hamiltonian writes:

---

\* sylvain.ravets@c2n.upsaclay.fr

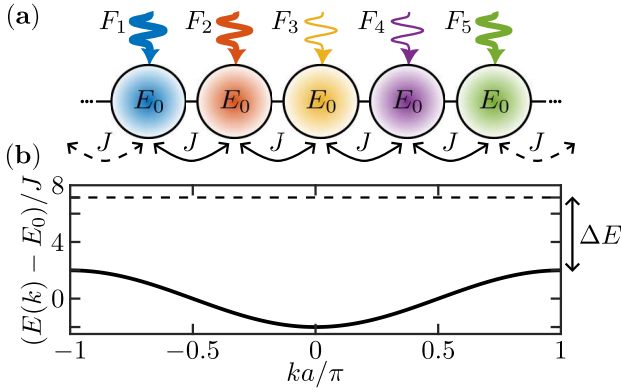


FIG. 1. a. Schematic of the lattice of coupled Kerr resonators. Each lattice site is individually driven (zigzag arrows). b. Energy dispersion of the lattice modes in the linear regime. The horizontal dashed line shows the energy  $\hbar\omega_P$  of the drives.

$$\hat{H} = \sum_n E_0 |\phi_n\rangle\langle\phi_n| - J (|\phi_n\rangle\langle\phi_{n+1}| + |\phi_n\rangle\langle\phi_{n-1}|), \quad (1)$$

where  $|\phi_n\rangle$  is the mode of resonator  $n$  with on-site energy  $E_0$ , and  $J$  is the coupling between neighboring sites. The eigenenergies of the Bloch eigenstates form a single band of dispersion  $E(k) = E_0 - 2J \cos(ka)$ , where  $a$  is the lattice period and  $k \in [-\pi/a, \pi/a]$  (see Fig. 1b). The nonlinear resonators are coherently driven by a monochromatic field oscillating at angular frequency  $\omega_P$ . The complex field amplitude at site  $n$  is  $F_n$ , and all sites experience a uniform loss rate  $\gamma$ . In the mean field approximation, the system dynamics is governed by the following driven-dissipative Gross Pitaevskii equation:

$$i\hbar\partial_t\psi = \left( \hat{H} - i\frac{\gamma}{2}\hat{\mathbb{1}} + g\hat{N} \right) \psi + i\mathbf{F}e^{-i\omega_P t}, \quad (2)$$

where  $g$  is the Kerr nonlinearity,  $\psi$  is a vector of components  $\psi_n$ ,  $\hat{N}$  is a diagonal operator with non-zero elements equal to  $\hat{N}_{n,n} = |\psi_n|^2$ ,  $\hat{\mathbb{1}}$  is the identity matrix, and  $\mathbf{F}$  is a vector of components  $F_n$ . In the rest of this letter, we define the energy detuning between the drive and the top of the band  $\Delta E = \hbar\omega_P - E_0 - 2J$  (see Fig. 1b), and the drive power  $P = \sum_n |F_n|^2$ .

We propose a drive protocol where we spatially modulate the pump amplitudes as follows:

$$F_n(\varphi) = F |\cos(\varphi/2 + \pi\alpha n)|, \quad (3)$$

where  $\alpha = 1/5$  and the parameter  $\varphi$  is a phason that can take values between 0 and  $2\pi$ . Note that the spatial periodicity of this protocol is  $5a$ , meaning that each unit cell of this drive pattern contains five sites.

We first set  $\varphi = 0$  and compute the system nonlinear steady-state versus  $P$ , solving Eq. 2. We plot, in Fig. 2a, the stationary field intensity pattern  $|\psi_n^{(s)}|^2$  calculated

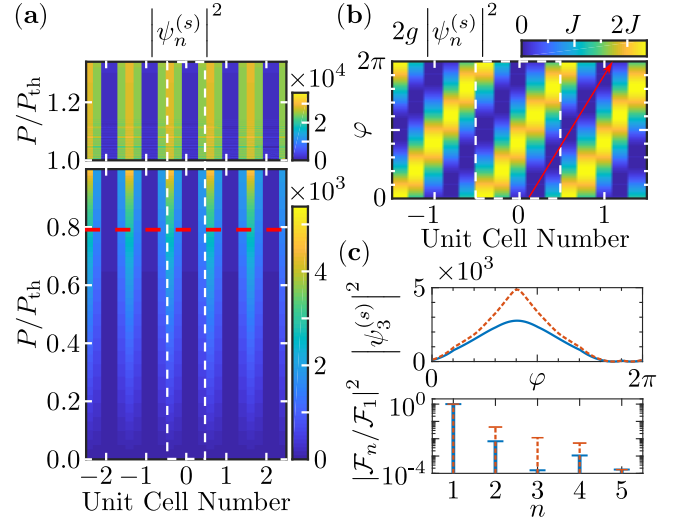


FIG. 2. a. Stationary intensity map versus unit cell number and power for the lattice driven according to  $\varphi = 0$  in Eq. 3. The dotted horizontal line marks the drive power  $P = 0.79P_{\text{th}}$  used in most part of this letter. b. Nonlinear onsite energies  $2g|\psi_n^{(s)}(F_n(\varphi))|^2$  as a function of  $\varphi$ . The red arrow is a guide to the eye to highlight the trajectory for one energy minimum. The vertical white dashed lines in a. and b. delimit the five sites forming one unit cell. c) Top panel: the population  $|\psi_3^{(s)}|^2$  on site 3 of the unit cell is shown as a function of  $\varphi$  for  $P/P_{\text{th}} = 0.79$  (solid blue line) and for  $P/P_{\text{th}} = 0.996$  (dashed red line). The associated power spectra (normalized to the power in the fundamental harmonic  $|F_1|^2$ ) are plotted in the bottom panel. The numerical parameters are  $\gamma = 44.7 \mu\text{eV}$ ,  $J/\gamma = 2.2$ ,  $g/\gamma = 10^{-3}$ ,  $\Delta E = 5.14J$ .

for increasing values of  $P$ . The intensity pattern follows the periodicity of the driving field, and evidences a nonlinear threshold at  $P = P_{\text{th}}$ , characteristic of a multi-stable nonlinear system. In the following, unless stated otherwise, we set  $P/P_{\text{th}} = 0.79$  (red dashed line in Fig. 2a).

We now compute the excitation spectrum on top of this nonlinear steady state. To do so, we use a Bogoliubov approach writing:  $\psi(t) = (\psi^{(s)} + \delta\psi(t))e^{-i\omega_P t}$ . Introducing this ansatz into the Gross-Pitaevskii equation, we obtain the following linearized equations for  $\delta\psi(t)$  and  $\delta\psi^*(t)$ :

$$i\hbar\partial_t \begin{pmatrix} \delta\psi(t) \\ \delta\psi^*(t) \end{pmatrix} = \begin{pmatrix} \hat{\mathcal{M}} & \hat{\mathcal{N}} \\ -\hat{\mathcal{N}}^* & -\hat{\mathcal{M}}^* \end{pmatrix} \begin{pmatrix} \delta\psi(t) \\ \delta\psi^*(t) \end{pmatrix}, \quad (4)$$

where  $\hat{\mathcal{M}} = \hat{H} - (\hbar\omega_P + i\frac{\gamma}{2})\hat{\mathbb{1}} + 2g\hat{N}^{(s)}$ , and  $\hat{\mathcal{N}}$  is a diagonal operator with non-zero elements equal to  $\hat{\mathcal{N}}_{n,n} = g(\psi_n^{(s)})^2$ .

The stationary solutions of Eq. 4 have the form:  $\delta\psi(t) = \mathbf{u}e^{-i\mathcal{E}t/\hbar} + \mathbf{v}^*e^{i\mathcal{E}^*t/\hbar}$ , where  $(\mathbf{u}, \mathbf{v})^T$  is an eigenvector of the Bogoliubov matrix written in Eq. 4 for the eigenvalue  $\mathcal{E}$ . The set of all possible  $\text{Re}(\mathcal{E})$  values gives

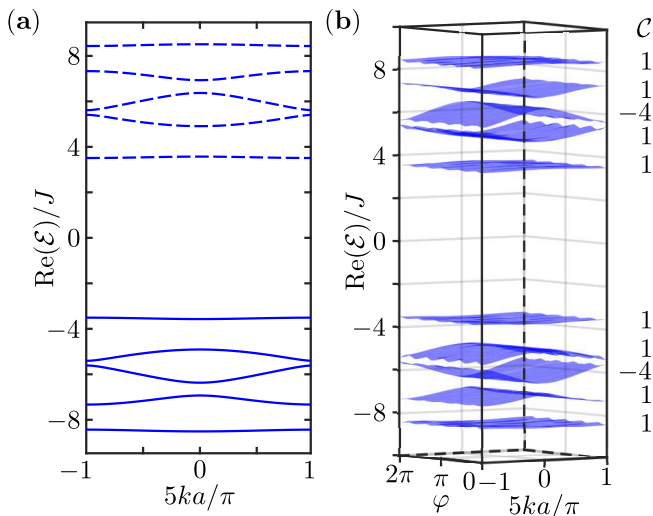


FIG. 3. a. Bogoliubov bands on top of the nonlinear steady-state  $\psi^{(s)}$ . The normal (ghost) branches are shown in solid (dashed) lines. b. 1+1D Bogoliubov bands as a function of  $k$  and  $\varphi$ . The computed Chern numbers are given aside each band.  $\gamma = 44.7 \mu\text{eV}$ ,  $J/\gamma = 2.2$ ,  $g/\gamma = 10^{-3}$ ,  $\Delta E = 5.14J$ ,  $P/P_{\text{th}} = 0.79$

rise to the Bogoliubov spectrum of excitations. It is convenient to write the Bogoliubov eigenmodes in reciprocal space versus wavevector  $k$ , using the basis of Bloch states  $(\tilde{\mathbf{u}}(k), \tilde{\mathbf{v}}(k))^T$ . For each site  $i$  of the unit cell,  $\tilde{\mathbf{u}}_i(k)$  and  $\tilde{\mathbf{v}}_i(k)$  are called the “normal” and “ghost” branch amplitudes.

Figure 3a shows the resulting Bogoliubov spectrum versus  $k$ . Because of the  $5a$  spatial period imposed by the drive,  $k$  takes values within  $]-\pi/5a, \pi/5a[$ . We clearly observe the presence of 10 bands separated by energy gaps. By construction, the bands are symmetric with respect to the pump energy  $\text{Re}(\mathcal{E}) = 0$  (particle-hole symmetry). The five low energy bands correspond to the “normal” modes ( $|\tilde{\mathbf{u}}(k)|^2 - |\tilde{\mathbf{v}}(k)|^2 = 1$ ), while the five upper energy bands correspond to the “ghost” modes ( $|\tilde{\mathbf{u}}(k)|^2 - |\tilde{\mathbf{v}}(k)|^2 = -1$ ). This spectrum highlights that spatially engineering the driving field enables tailoring the Bogoliubov band structure [26].

We now consider a protocol where  $\varphi$  is adiabatically varied between 0 and  $2\pi$ . As we vary  $\varphi$ , the diagonal elements of the Bogoliubov matrix are periodically modulated according to  $\hat{\mathcal{M}}_{n,n}(\varphi) = E_0 + 2g \left| \psi_n^{(s)}(F_n(\varphi)) \right|^2 - (\hbar\omega_P + i\frac{\gamma}{2})$ . Strikingly,  $\hat{\mathcal{M}}$  has the form of an Aubry-André-Harper Hamiltonian [34, 35], where the onsite energies are modulated as a function of  $\varphi$ , while the coupling coefficients  $J$  stay constant. As highlighted in Ref. [7, 36], one can see  $\varphi$  as a parametric dimension in a 1+1D space. Every realization of  $\hat{\mathcal{M}}(\varphi)$  is a Fourier component of a 2D operator  $\hat{\mathcal{M}}_{2D}$  acting on the 1+1D system. For a pure sine-modulation of the on-site energies,  $\hat{\mathcal{M}}_{2D}$  exactly coincides with the Harper-Hofstadter

Hamiltonian [37] describing particles on a square lattice with a non-zero flux per plaquette equal to  $2\pi\alpha$ .

In Fig. 2b, we show the nonlinear potential  $2g \left| \psi_n^{(s)}(F_n(\varphi)) \right|^2$  evolution versus  $\varphi$ . We observe that it defines a series of potential wells that get deformed as we vary  $\varphi$ , in a way that they exhibit a unidirectional motion, as expected for an adiabatic pump. The nonlinear response of the Kerr resonators leads to anharmonic modulations of the nonlinear onsite energies, so that the mapping to the Harper-Hofstadter Hamiltonian is not exact. This is illustrated in Fig. 2c, where  $\left| \psi_3^{(s)} \right|^2$  (population in the third site of the unit cell) is plotted for  $P/P_{\text{th}} = 79\%$  (blue solid line) and  $P/P_{\text{th}} = 99.6\%$  (red dashed). The corresponding power spectra are shown on the lower panel, where we evidence the increase of the anharmonicity as  $P$  approaches  $P_{\text{th}}$  from below. We show in the following that the band structure topology of the Harper-Hofstadter model persists as long as  $P/P_{\text{th}} < 99.6\%$ , illustrating its robustness against anharmonicities in the potential.

We plot, in Fig. 3b, the 1+1D (versus  $k$  and  $\varphi$ ) Bogoliubov energy bands outlined during the drive protocol. We observe that all gaps described in Fig. 2 remain open for all  $\varphi$  values. For the five normal and the five ghost branches, we then compute Chern numbers [38, 39] and find  $\mathcal{C} = 1, 1, -4, 1, 1$ . These values correspond to the Chern numbers expected for the Harper-Hofstadter model with magnetic flux  $\alpha = 1/5$ . Adjusting the drive protocol, we point out that one can straightforwardly extend this demonstration to any rational flux  $\alpha = p/q$ , where  $q$  is the number of sites per unit cell. These results establish adiabatic drive modulation of a nonlinear fluid of light as a powerful tool to induce non-trivial topology in an effectively 2D space with one synthetic parametric dimension.

To evidence topological pumping for the Bogoliubov excitations, we now investigate the Wannier centers and their evolution during the drive protocol. For every value of  $\varphi$ , we compute the maximally-localized Wannier states associated to the five lowest energy (“normal”) bands. For each normal band, we show in Fig 4, the intensity distribution  $|u_n|^2$  of the Wannier state located at a chosen unit cell, and we monitor its evolution as a function of  $\varphi$ . The solid lines follow the barycenter trajectories for these Wannier states, and clearly highlight a net motion of the Wannier centers. Moreover, after one modulation period, each Wannier state has moved by a quantized number of unit cells that exactly matches the Chern number of the band. This fully demonstrates that we have realized a topological pump for Bogoliubov excitations. The crucial novelty of our result lies in the fact that the pumping mechanism relies entirely on the presence of inter-particle interactions which modulate the potential acting on Bogoliubov excitations.

So far, we have focused on a value of  $P$  lying well below  $P_{\text{th}}$ . As discussed in Fig. 2c, the nonlinear character of the modulation protocol, leads to power depen-

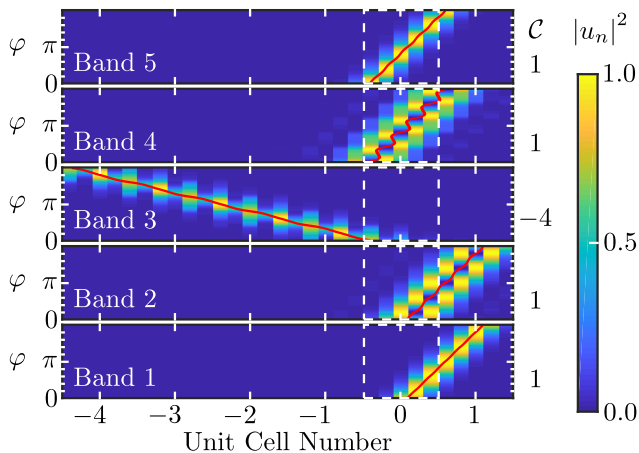


FIG. 4. Intensity distributions  $|u_n|^2$  of a Wannier state located at a chosen lattice position as a function of  $\varphi$ . From bottom to top, we represent Wannier states in each of the five normal bands ordered by increasing energies. The red lines trace the barycenter motion of each Wannier state during one protocol period. The white dashed lines delimit one unit cell. The intensity distributions are normalized to their maximum values. All numerical parameters are identical to the ones used in Fig. 3.

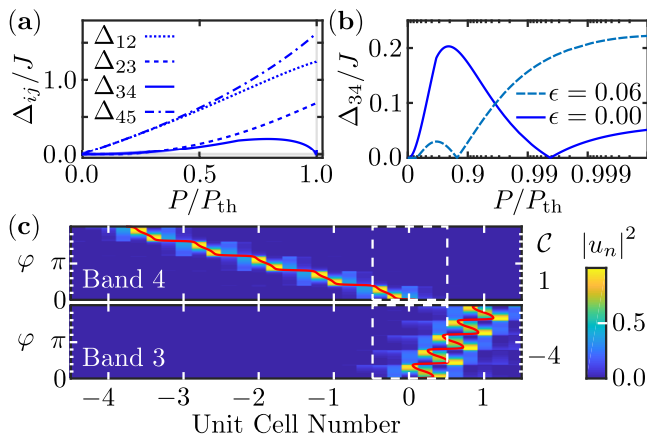


FIG. 5. a. Energy gaps  $\Delta_{ij}$  versus  $P/P_{\text{th}}$ . b. Logarithmic plot of  $\Delta_{34}/J$  versus  $P/P_{\text{th}}$  for  $\epsilon = 0$  (solid line) and  $\epsilon = 0.06$  (dashed line). c. Intensity distributions  $|u_n|^2$  versus  $\varphi$  for the Wannier states associated to the third (bottom) and fourth (top) Bogoliubov bands obtained for  $\epsilon = 0$ , just below  $P_{\text{th}}$  ( $P/P_{\text{th}} = 99.99\%$ ). The red lines trace the barycenter motion of each Wannier state during one protocol period. The intensity distributions are normalized to their maximum values.

dent anharmonicities in the modulated onsite energies. In Figure 5a, we plot the evolution of the energy gaps  $\Delta_{ij}$  between bands  $i$  and  $j$ , as we increase  $P$  up to  $P_{\text{th}}$ . Interestingly, at a critical power  $P_c/P_{\text{th}} = 99.6\%$ , we observe that  $\Delta_{34}$  vanishes, and then the gap reopens (see semi-logarithmic plot in Fig. 5b). For power values within the range ( $P_c < P < P_{\text{th}}$ ), we repeat our analysis of the resulting pump. We first compute the

Chern numbers for the 1+1D Bogoliubov bands, and obtain  $\mathcal{C} = 1, 1, 1, -4, 1$ . Compared to the situation discussed previously in Fig. 3b, we do not recover the same Chern number ordering, as the Chern numbers of the third and fourth bands are inverted. We then calculate the Wannier centers evolution and find that their barycenter motion follows the new Chern number ordering. Indeed, the Wannier state motions in the third and fourth bands (see Fig. 5c), are inverted as compared to Fig. 4, while the motions stay unchanged in the rest of the bands (not shown). These results evidence the occurrence of a topological transition induced by the nonlinearity and the resulting anharmonic modulation of the onsite energies. We note that the  $n$ th harmonic introduces nonzero  $n$ th-neighbor coupling in the parametric dimension, so that deviations in the mapping to the 2D Harper-Hofstadter model without long range couplings can no longer be neglected, and the system experiences a topological transition.

Increasing  $P$  to values  $P > P_{\text{th}}$ , we observe that the anharmonicity of the onsite energy modulation decreases, and we recover the Harper-Hofstadter Chern ordering. These results illustrate an asset of our pump protocol, whereby the drive amplitude can be used as a knob to control the topology that emerges in the Bogoliubov spectrum, in a way that Bogoliubov excitations experience topological transitions. As a further tuning knob, we now show that one can control  $P_c$  by modifying the frequency spectrum of the drive protocol. We illustrate this feature by studying the evolution of  $\Delta_{34}$  versus  $P/P_{\text{th}}$  when adding a second order harmonic to the drive:

$$F_n(\varphi) = F |\cos(\varphi/2 + \pi\alpha n)| + \epsilon F |\cos(\varphi + 2\pi\alpha n)|. \quad (5)$$

The result is shown in Fig. 5b (dashed line) for  $\epsilon = 0.06$ . Under the modified drive protocol, the critical power at which the topological transition occurs gets significantly reduced to the value  $P'_c = 0.85P'_{\text{th}}$ . This confirms that the observed gap closure and ensuing topological transition are rooted in the evolution of modulation anharmonicities as the nonlinearity develops. We note that tuning the number and amplitudes of harmonics included in the drive protocol provides a vast nonlinear optics framework to trigger topological transitions and control the motion of Wannier states in the Bogoliubov excitation spectrum. A systematic study of these effects is beyond the scope of this letter.

In conclusion, starting with a trivial lattice of driven-dissipative Kerr resonators, we establish Bogoliubov excitations as a playground to organize Thouless pumping through spatial engineering of the drive. Adiabatically modulating the drive pattern introduces a parametric dimension leading to 1+1D topological bands. As a consequence of the presence of non-zero Chern numbers, the Bogoliubov Wannier states associated to the bands experience quantized motion through Thouless pumping. Moreover, the nonlinearity modifies the frequency spectrum of the onsite energy modulation, leading to topological transitions that switch the directionality and am-

plitude of the quantized motion of Wannier states within different bands. We emphasize that all our simulations are performed using realistic parameters that are compatible with the exciton polariton platform. Benefiting from recent progress in probing and manipulating Bogoliubov excitations in these systems [32, 33, 40], we foresee that the experimental implementation of the proposed topological pump is within reach. As a further development, we envision that drive engineering can be used to induce uniform magnetic flux for Bogoliubov excitations in 2D lattices. By extending the perturbative approach of Ref. [26], one could realize Hofstadter-type models with large synthetic flux  $\Phi \sim \pi$  per plaquette, hence offering new opportunities to explore nonlinear topology in 2D lattices [41, 42].

### ACKNOWLEDGMENTS

We thank A. Amo, I. Carusotto, and O. Zilberberg for fruitful discussions. This work was partly supported

by the Paris Ile de France Région in the framework of DIM SIRTEQ, by the European Research Council (ERC) under the European Union's Horizon 2020 research and innovation programme (project ARQADIA, grant agreement no. 949730), and under Horizon Europe research and innovation programme (ANAPOLIS, grant agreement no. 101054448). NG is supported by the ERC Grant LATIS and the EOS project CHEQS. NM acknowledges funding by the Deutsche Forschungsgemeinschaft (DFG, German Research Foundation) under Germany's Excellence Strategy – EXC-2111 – 390814868.

- 
- [1] D. J. Thouless, Quantization of particle transport, *Phys. Rev. B* **27**, 6083 (1983).
- [2] R. Citro and M. Aidelsburger, Thouless pumping and topology, *Nature Reviews Physics* **5**, 87 (2023).
- [3] M. Lohse, C. Schweizer, O. Zilberberg, M. Aidelsburger, and I. Bloch, A Thouless quantum pump with ultracold bosonic atoms in an optical superlattice, *Nature Physics* **12**, 350 (2016).
- [4] S. Nakajima, T. Tomita, S. Taie, T. Ichinose, H. Ozawa, L. Wang, M. Troyer, and Y. Takahashi, Topological Thouless pumping of ultracold fermions, *Nature Physics* **12**, 296 (2016).
- [5] H.-I. Lu, M. Schemmer, L. M. Aycock, D. Genkina, S. Sugawa, and I. B. Spielman, Geometrical pumping with a bose-einstein condensate, *Phys. Rev. Lett.* **116**, 200402 (2016).
- [6] D. Dreon, A. Baumgärtner, X. Li, S. Hertlein, T. Esslinger, and T. Donner, Self-oscillating pump in a topological dissipative atom-cavity system, *Nature* **608**, 494 (2022).
- [7] Y. E. Kraus, Y. Lahini, Z. Ringel, M. Verbin, and O. Zilberberg, Topological states and adiabatic pumping in quasicrystals, *Phys. Rev. Lett.* **109**, 106402 (2012).
- [8] Y. Ke, X. Qin, F. Mei, H. Zhong, Y. S. Kivshar, and C. Lee, Topological phase transitions and thouless pumping of light in photonic waveguide arrays, *Laser & Photonics Reviews* **10**, 995 (2016).
- [9] A. Cerjan, M. Wang, S. Huang, K. P. Chen, and M. C. Rechtsman, Thouless pumping in disordered photonic systems, *Light: Science & Applications* **9**, 178 (2020).
- [10] Z. Fedorova, H. Qiu, S. Linden, and J. Kroha, Observation of topological transport quantization by dissipation in fast Thouless pumps, *Nature Communications* **11**, 3758 (2020).
- [11] I. H. Grinberg, M. Lin, C. Harris, W. A. Benalcazar, C. W. Peterson, T. L. Hughes, and G. Bahl, Robust temporal pumping in a magneto-mechanical topological insulator, *Nature Communications* **11**, 974 (2020).
- [12] Y. Xia, E. Riva, M. I. N. Rosa, G. Cazzulani, A. Erturk, F. Braghin, and M. Ruzzene, Experimental observation of temporal pumping in electromechanical waveguides, *Phys. Rev. Lett.* **126**, 095501 (2021).
- [13] Q. Niu and D. J. Thouless, Quantised adiabatic charge transport in the presence of substrate disorder and many-body interaction, *Journal of Physics A: Mathematical and General* **17**, 2453 (1984).
- [14] Y. Kuno and Y. Hatsugai, Interaction-induced topological charge pump, *Phys. Rev. Res.* **2**, 042024(R) (2020).
- [15] K. Viebahn, A.-S. Walter, E. Bertok, Z. Zhu, M. Gächter, A. A. Aligia, F. Heidrich-Meisner, and T. Esslinger, Interaction-induced charge pumping in a topological many-body system (2023), [arXiv:2308.03756 \[cond-mat.quant-gas\]](https://arxiv.org/abs/2308.03756).
- [16] T. Tuloup, R. W. Bomantara, and J. Gong, Breakdown of quantization in nonlinear thouless pumping (2023), in press.
- [17] A.-S. Walter, Z. Zhu, M. Gächter, J. Minguzzi, S. Roschinski, K. Sandholzer, K. Viebahn, and T. Esslinger, Quantization and its breakdown in a Hubbard-Thouless pump, *Nature Physics* **10.1038/s41567-023-02145-w** (2023).
- [18] M. Jürgensen, S. Mukherjee, and M. C. Rechtsman, Quantized nonlinear thouless pumping, *Nature* **596**, 63 (2021).
- [19] M. Jürgensen and M. C. Rechtsman, Chern number governs soliton motion in nonlinear thouless pumps, *Physical review letters* **128**, 113901 (2022).
- [20] N. Mostaan, F. Grusdt, and N. Goldman, Quantized topological pumping of solitons in nonlinear photonics and ultracold atomic mixtures, *Nature Communications* **13**, 5997 (2022).
- [21] Q. Fu, P. Wang, Y. V. Kartashov, V. V. Konotop, and

- F. Ye, Nonlinear thouless pumping: Solitons and transport breakdown, *Phys. Rev. Lett.* **128**, 154101 (2022).
- [22] M. Jürgensen, S. Mukherjee, C. Jörg, and M. C. Rechtsman, Quantized fractional thouless pumping of solitons, *Nature Physics* **19**, 420 (2023).
- [23] Y. Ke, X. Qin, Y. S. Kivshar, and C. Lee, Multiparticle wannier states and thouless pumping of interacting bosons, *Phys. Rev. A* **95**, 063630 (2017).
- [24] J. Tangpanitanon, V. M. Bastidas, S. Al-Assam, P. Roushan, D. Jaksch, and D. G. Angelakis, Topological pumping of photons in nonlinear resonator arrays, *Phys. Rev. Lett.* **117**, 213603 (2016).
- [25] N. N. Bogoliubov, On the theory of superfluidity, *J.Phys.(USSR)* **11**, 23 (1947).
- [26] C.-E. Bardyn, T. Karzig, G. Refael, and T. C. H. Liew, Chiral bogoliubov excitations in nonlinear bosonic systems, *Phys. Rev. B* **93**, 020502(R) (2016).
- [27] M. Di Liberto, A. Hemmerich, and C. Morais Smith, Topological vortices superfluid in optical lattices, *Phys. Rev. Lett.* **117**, 163001 (2016).
- [28] I. Carusotto and C. Ciuti, Quantum fluids of light, *Rev. Mod. Phys.* **85**, 299 (2013).
- [29] C. Schneider, K. Winkler, M. D. Fraser, M. Kamp, Y. Yamamoto, E. A. Ostrovskaya, and S. Höfling, Exciton-polariton trapping and potential landscape engineering, *Reports on Progress in Physics* **80**, 016503 (2016).
- [30] V. Kohnle, Y. Léger, M. Wouters, M. Richard, M. T. Portella-Oberli, and B. Deveaud-Plédran, From single particle to superfluid excitations in a dissipative polariton gas, *Phys. Rev. Lett.* **106**, 255302 (2011).
- [31] J. M. Zajac and W. Langbein, Parametric scattering of microcavity polaritons into ghost branches, *Phys. Rev. B* **92**, 165305 (2015).
- [32] P. Stepanov, I. Amelio, J.-G. Rousset, J. Bloch, A. Lemaître, A. Amo, A. Minguzzi, I. Carusotto, and M. Richard, Dispersion relation of the collective excitations in a resonantly driven polariton fluid, *Nature Communications* **10**, 3869 (2019).
- [33] F. Claude, M. J. Jacquet, R. Usciati, I. Carusotto, E. Giacobino, A. Bramati, and Q. Glorieux, High-resolution coherent probe spectroscopy of a polariton quantum fluid, *Phys. Rev. Lett.* **129**, 103601 (2022).
- [34] P. G. Harper, Single band motion of conduction electrons in a uniform magnetic field, *Proceedings of the Physical Society. Section A* **68**, 874 (1955).
- [35] S. Aubry and G. André, Analyticity breaking and anderson localization in incommensurate lattices, *Ann. Israel Phys. Soc* **3**, 133 (1980).
- [36] Y. E. Kraus and O. Zeitler, Topological equivalence between the fibonacci quasicrystal and the harper model, *Phys. Rev. Lett.* **109**, 116404 (2012).
- [37] D. R. Hofstadter, Energy levels and wave functions of bloch electrons in rational and irrational magnetic fields, *Phys. Rev. B* **14**, 2239 (1976).
- [38] V. Peano, M. Houde, C. Brendel, F. Marquardt, and A. A. Clerk, Topological phase transitions and chiral inelastic transport induced by the squeezing of light, *Nature Communications* **7**, 10779 (2016).
- [39] The Chern numbers are obtained by integrating the Berry curvature of Bogoliubov bands, taking into account their intrinsic symplectic structure, see Ref. [38].
- [40] I. Frérot, A. Vashishta, M. Morassi, A. Lemaître, S. Ravets, J. Bloch, A. Minguzzi, and M. Richard, Bogoliubov excitations driven by thermal lattice phonons in a quantum fluid of light, *Phys. Rev. X* **13**, 041058 (2023).
- [41] I. Tesfaye and A. Eckardt, *Quantum geometry of bosonic bogoliubov quasiparticles* (2024), [arXiv:2406.12981 \[cond-mat.quant-gas\]](https://arxiv.org/abs/2406.12981).
- [42] G. Villa, J. del Pino, V. Dumont, G. Rastelli, M. Michałek, A. Eichler, and O. Zeitler, *Topological classification of driven-dissipative nonlinear systems* (2024), [arXiv:2406.16591 \[cond-mat.mes-hall\]](https://arxiv.org/abs/2406.16591).